Contribution from the Department of Chemistry, Northwestern University, Evanston, Illinois 60208

Anionic Iron Carbido Carbonyl Clusters with Sulfur Dioxide Ligands

P. L. Bogdan, M. Sabat, S. A. Sunshine, C. Woodcock, and D. F. Shriver*

Received December 29, 1987

The reactions of sulfur dioxide with salts of a series of anionic carbido carbonyl clusters $[Fe_n(CO)_xC]^{2-}$ (n = 3–6, x = 10, 12, 14, 16) were investigated. Substitution of SO_2 for one CO ligand occurs with the $[Fe_6(CO)_{16}C]^{2-}$ anion to produce the $[Fe_6(CO)_{15}C(SO_2)]^{2-}$ anion in high yield. Substitution is the primary reaction when the $[Fe_5(CO)_{14}C]^{2-}$ anion takes up SO_2 to give $[Fe_5(CO)_{13}C(SO_2)]^{2-}$, but some cluster oxidation also occurs. An oxidative degradation results when salts of $[Fe_4(CO)_{12}C]^{2-}$ are treated with 4 mol of SO_2, and the products are salts of the bis(sulfur dioxide)-substituted triiron ketenylidene cluster $[Fe_3(CO)_7(CCO)(SO_2)_2]^{2-}$. The products of these reactions were characterized by spectroscopy and by single-crystal X-ray diffraction. Sulfur dioxide oxidized the triiron cluster $[Fe_3(CO)_9(CCO)]^{2-}$ to a complex mixture of carbonyl-containing species. The reactivity of the iron carbido carbonyl cluster anions can be rationalized on the basis of redox potentials determined by cyclic voltammetry, which reflect the negative charge/metal ratio. The spectroscopic data indicate that SO_2 behaves as a stronger electron acceptor ligand than CO toward these clusters. Crystal data for $[(PhCH_2)NMe_3]_2[Fe_6(CO)_{15}C(SO_2)]$: orthorhombic, space group $Pna2_1$; a = 14.642 (2), b = 15.142 (2), c = 19.329 (3) Å; final R = 4.5%, R_w = 4.2%. Crystal data for $[PPN]_2[Fe_5(CO)_{13}C(SO_2)]$: monoclinic, space group $P2_1/c$; a = 19.384 (5), b = 15.644 (6), c = 26.612 (4) Å; β = 103.03 (2)°; final R = 5.8%, R_w = 7.3%. Crystal data for $[EtPr_3N]_2[Fe_3(CO)_7(CCO)(SO_2)_2]$: monoclinic, space group $P2_1/n$; a = 10.978 (3), b = 22.359 (4), c = 16.810 (3) Å; β = 90.10 (2)°; final R = 6.6%, R_w = 6.9%.

Introduction

Sulfur dioxide is an interesting ligand that can function as either a Lewis base or a Lewis acid toward a metal center. A large number of mononuclear metal complexes containing sulfur dioxide have been synthesized.[1,2] These compounds have been the subject of numerous structural, spectroscopic, and theoretical studies.[1–6] The bonding mode and positions of the S–O stretches in the infrared region are often useful probes into the electronic environment at the metal center.[3]

In contrast, relatively few metal cluster compounds containing sulfur dioxide have been synthesized. The majority of these are trinuclear palladium and platinum clusters.[7] Other larger clusters have been prepared, such as $Pt_5(CO)_3(SO_2)_3(PPh_3)_4$[8] and $Ir_4(CO)_{11}(SO_2)$.[9] The only iron-subgroup SO_2 cluster reported to date is $H_2Os_3(CO)_{10}(SO_2)$.[10] All of these clusters contain SO_2 as a 2e-donor ligand, with the S atom bridging two metal centers. An exception is $Rh_4(CO)_4(P(OPh_3))_4(SO_2)_3$, which contains two μ_3-η^2-SO_2 ligands that donate 4e to the cluster.[11]

Interest in sulfur dioxide substituted carbonyl clusters is 2-fold. Research efforts have centered on the multicenter activation of small molecules on clusters, since it was observed that the activation of CO by a four-iron cluster can lead to the formation of carbide clusters[12] and, under forcing conditions, to methane.[13] An intriguing possibility would be to try to effect S–O bond activations in a similar manner. It is also of interest to contrast the properties of carbonyl and sulfur dioxide ligands for anionic clusters. The similarities and differences of these two ligands bound to mononuclear complexes have been highlighted by theoretical and spectroscopic studies.[1,2,5,14] Comparison of bridging CO and SO_2 on metal cluster compounds has received far less attention.[6]

The present investigation of the reaction of SO_2 with the salts of a series of dinegative iron carbido carbonyl clusters containing three to six iron atoms has led to the synthesis and characterization of several new anionic clusters containing sulfur dioxide ligands. Only one other anionic cluster containing the SO_2 ligand has been reported.[15]

Experimental Section

General Procedures. All manipulations were performed under air- and moisture-free conditions by using standard Schlenk and vacuum-line techniques. Solvents were dried and distilled under an atmosphere of prepurified N_2 before use: CH_2Cl_2 was distilled from P_2O_5, i-Pr_2O, Et_2O, and THF were distilled from sodium benzophenone ketyl, and toluene was distilled from sodium. $[PPN]_2[Fe_3(CO)_9(CCO)]$,[16] $[PPN]_2[Fe_4(CO)_{12}C]$,[17] $[PPN]_2[Fe_5(CO)_{14}C]$,[18] and $[PPN]_2[Fe_6(CO)_{16}C]$[19] were prepared by literature methods. (PPN^+ is the abbreviation for (μ-nitrido)bis(triphenylphosphorus)(1+).) Compounds enriched in ^{13}CO were prepared as follows: $[PPN]_2[Fe_3(*CO)_9(*C*CO)]$ from $[PPN]_2[Fe_3(CO)_{11}]$ enriched by two cycles of stirring under 80 Torr of 99% ^{13}CO in CH_3CN for 90 min each and $[PPN]_2[Fe_4(*CO)_{12}*C]$ from $[PPN]_2[Fe_4(CO)_{13}]$ enriched by stirring in CH_2Cl_2 under 1 atm of 99% ^{13}CO for 5 days. The six-metal cluster, $[PPN]_2[Fe_6(*CO)_{16}*C]$, was synthesized by addition of excess $Fe_2(CO)_9$ to a THF slurry of $[PPN]_2[Fe_3(*CO)_9(*C*CO)]$, followed by filtration and crystallization from THF/Et_2O. The ^{13}C NMR spectra for derivatives of $[PPN]_2[Fe_5(CO)_{14}C]$ were obtained on unenriched samples. Chemical shifts are based on δ(TMS) = 0 and were measured relative to the solvent.

Infrared spectra were recorded on a Perkin-Elmer 283 or Nicolet 7900 FT-IR instrument. NMR spectra were obtained on a JEOL FX-270 or Varian XL-400 spectrometer with $Cr(acac)_3$ added as a shiftless relaxation agent. Elemental analyses were performed by Galbraith Laboratories. Cyclic voltammograms were recorded of samples placed in an airtight one-compartment cell equipped with a platinum-disk working electrode (1.6-mm diameter), a platinum-loop auxiliary electrode, and a silver-wire reference electrode immersed in electrolyte solution and isolated from the other electrodes by a 5-mm glass tube containing an asbestos-fiber barrier. The potential of the silver-wire reference was

(1) Ryan, R. R.; Kubas, G. J.; Moody, D. C.; Eller, P. G. *Struct. Bonding (Berlin)* 1981, 46, 47.
(2) Mingos, D. M. P. *Transition Met. Chem. (Weinheim, Ger.)* 1978, 3, 1.
(3) Kubas, G. J. *Inorg. Chem.* 1979, 18, 182.
(4) Ryan, R. R.; Eller, P. G. *Inorg. Chem.* 1976, 5, 494.
(5) Schilling, B. E. R.; Hoffmann, R.; Lichtenberger, D. L. *J. Am. Chem. Soc.* 1979, 101, 585.
(6) Gilmour, D. I.; Mingos, D. M. P. *J. Organomet. Chem.* 1986, 302, 127.
(7) (a) Otsuka, S.; Tatsuno, Y.; Aoki, T.; Matsumoto, M.; Yoshioko, H.; Nakatsu, K. *J. Chem. Soc., Chem. Commun.* 1973, 445. (b) Werner, K. V.; Beck, W.; Bohner, U. *Chem. Ber.* 1974, 107, 2434. (c) Moody, D. C.; Ryan, R. R. *Inorg. Chem.* 1977, 16, 1052. (d) Evans, D. G.; Hughes, G. R.; Mingos, D. M. P.; Basset, J.-M.; Welch, A. J. *J. Chem. Soc., Chem. Commun.* 1980, 1225. (e) Browning, C. S.; Farrar, D. H.; Gukathason, R. R.; Morris, S. A. *Organometallics* 1985, 4, 1750. (f) Mingos, D. M. P.; Wardle, R. W. M. *J. Chem. Soc., Dalton Trans.* 1986, 73. (g) Mingos, D. M. P.; Oster, P.; Sherman, D. J. *J. Organomet. Chem.* 1987, 320, 257.
(8) Briant, C. E.; Evans, D. G.; Mingos, D. M. P. *J. Chem. Soc., Chem. Commun.* 1982, 1144.
(9) Braga, D.; Ros, R.; Roulet, R. *J. Organomet. Chem.* 1985, 286, C8.
(10) Jarvinen, G. D.; Ryan, R. R. *Organometallics* 1984, 3, 1434.
(11) Briant, C. E.; Theobald, B. R. C.; Mingos, D. M. P. *J. Chem. Soc., Chem. Commun.* 1981, 963.
(12) Holt, E. M.; Whitmire, K. H.; Shriver, D. F. *J. Organomet. Chem.* 1981, 213, 215.
(13) Drezdzon, M. A.; Shriver, D. F. *J. Mol. Catal.* 1983, 21, 81.
(14) Blevins, C. H., II. Ph.D. Dissertation, University of Arizona, 1984.
(15) Hallam, M. F.; Mingos, D. M. P. *J. Organomet. Chem.* 1986, 315, C35.
(16) Kolis, J. W.; Holt, E. M.; Shriver, D. F. *J. Am. Chem. Soc.* 1983, 105, 7307.
(17) Kolis, J. W.; Drezdzon, M. A.; Shriver, D. F. *Inorg. Synth.*, in press.
(18) Lopatin, V. E.; Mikova, N. M.; Gubin, S. P. *Izv. Akad. Nauk SSSR, Ser. Khim.* 1983, 6, 1407.
(19) Tachikawa, M.; Geerts, R. L.; Muetterties, E. L. *J. Organomet. Chem.* 1981, 213, 11.

0020-1669/88/1327-1904$01.50/0

periodically checked against ferrocene. A Princeton Applied Research Model 373 potentiostat/galvanostat with an in-house-built digital controller was used. The program ICON8 was used in extended Hückel molecular orbital calculations.[20] Atomic parameters were taken from ref 21.

Preparation of $[PPN]_2[Fe_3(CO)_7(CCO)(SO_2)_2]$. Excess SO_2 was condensed at −196 °C onto a 30-mL freeze–thaw-degassed CH_2Cl_2 solution of 0.70 g of $[PPN]_2[Fe_4(CO)_{12}C]$. The flask was warmed to room temperature, and its contents were stirred for several hours; then the flask was recooled to −196 °C, reevacuated, and rewarmed to room temperature. The color of the solution turned from deep brown to red-orange during the reaction period. After being stirred for an additional hour, the solution was filtered and layered with Et_2O (40 mL). Bright red crystalline flakes were collected by filtration and dried. Yield: 0.55 g, 80%. IR, CH_2Cl_2: 2045 m, 2004 s, 1983 s, 1943 m, 1811 w cm^{-1} (CO). IR, Nujol mull: 1175 m, 1042 m, 1028 s cm^{-1} (SO). ^{13}C NMR, −90 °C, in 20% CD_2Cl_2: δ 257.0 (μ-CO), 213.6 (1 CO), 211.7 (2 CO), 209.3 (2 CO), 209.0 (1 CO), 167.4 (C*C*O), 6.6 (*C*CO). Anal. Calcd for $C_{81}H_{60}N_2O_{12}Fe_3P_4S_2$: C, 60.47; H, 3.76; Fe, 10.41; S, 3.99. Found: C, 58.30, 57.95; H, 3.96, 3.55; Fe, 9.43, 10.48; S, 4.35, 4.42. The PPN^+ salt of this compound is soluble in CH_2Cl_2 and CH_3CN, is insoluble in THF, DME, *i*-PrOH, toluene, and methylcyclohexane, and decomposes in MeOH. Single crystals of the PPN^+ salt did not diffract X-rays. In an attempt to prepare crystals that were suitable for X-ray single-crystal structural investigation, the following salts of the cluster anion were investigated: $(PhCH_2)Me_3N^+$, $MePh_3P^+$, Ph_4P^+, Et_4N^+, K^+. However, none of these salts produced suitable single crystals. Single crystals that gave usable X-ray diffraction data were finally obtained with the $EtPr_3N^+$ cation. The reaction of $[EtPr_3N]_2[Fe_4(CO)_{12}C]$ was carried out analogously to that of the PPN^+ salt, except that THF was used as the reaction solvent, and toluene was substituted for Et_2O in the layering step. Single crystals were obtained by slow diffusion of Et_2O into a THF solution of $[EtPr_3N]_2[Fe_3(CO)_7(CCO)(SO_2)_2]$.

Preparation of $[PPN]_2[Fe_6(CO)_{15}C(SO_2)]$. To a freeze–thaw-degassed solution of CH_2Cl_2, 20 mL, containing 0.40 g of $[PPN]_2[Fe_6(CO)_{16}C]$ was added 1.3 equiv of SO_2 at −196 °C. After the solution was stirred at room temperature for 3.5 h, the evolution of 1.07 equiv of CO gas was measured by *PVT* methods. Further addition of SO_2 (1.4 equiv) in the same manner produced no further CO evolution. Dark purple crystals were obtained by layering 30 mL of Et_2O over the CH_2Cl_2 solution. Yield: 0.36 g, 87%. IR, CH_2Cl_2: 2040 w, 1982 vs, 1777 w cm^{-1} (CO). IR, Nujol mull: 1180 m, 1045 s (SO); 806 w cm^{-1} (Fe–C). ^{13}C NMR, −85 °C, in 20% CD_2Cl_2: δ 221 (br, CO), 480.1 (C). Single crystals of the PPN^+ salt of this compound diffracted X-rays weakly and belong to the monoclinic crystal system with a *C*-centered lattice. Due to the large number of non-hydrogen atoms to be located and refined in this salt, a crystal structure determination was not carried out on this crystal, and other salts were prepared. $[(PhCH_2)Me_3N]_2[Fe_6(CO)_{15}C(SO_2)]$ was synthesized by bubbling excess SO_2 gas through a THF solution of $[(PhCH_2)Me_3N]_2[Fe_6(CO)_{16}C]$ and crystallized by layering the THF solution with Et_2O. Single crystals suitable for X-ray analysis were obtained by slow diffusion of *i*-Pr_2O into a THF solution of the compound. Anal. Calcd for $C_{36}H_{32}N_2O_{17}Fe_6S$: C, 38.20; H, 2.85; Fe, 29.61; S, 2.83. Found: C, 38.37; H, 2.82; Fe, 29.79; S, 2.99.

Preparation of $[PPN]_2[Fe_5(CO)_{13}C(SO_2)]$. To 20 mL of a freeze–thaw-degassed solution of CH_2Cl_2 containing 0.40 g of $[PPN]_2[Fe_5(CO)_{14}C]$ was added 2.8 equiv of SO_2 at −196 °C. After the mixture was stirred at room temperature for about 4 h, sulfur dioxide gas was bubbled into the brown solution for a few minutes, and the resulting solution was filtered. Black crystals were obtained by layering 30 mL of Et_2O over the CH_2Cl_2 solution. Yield: 0.31 g, 76%. When the reaction was performed in the same manner using 0.3 g of $[PPN]_2[Fe_5(CO)_{14}C]$ and 1.1 equiv of SO_2 and worked up after stirring overnight, the yield was 0.17 g, 56%. IR, CH_2Cl_2: 2036 w, 1981 vs, 1972 sh, 1966 s, 1940 sh cm^{-1} (CO). IR, Nujol mull: 1028 s (SO); 817 w, 793 w cm^{-1} (Fe–C). ^{13}C NMR, +22 °C, in 20% CD_2Cl_2: δ 220.4, 219.7, 219.3, 212.1 (ca. 3:2:6:2) (CO), 475.0 (μ-C). Anal. Calcd for $C_{34}H_{32}N_2O_{15}Fe_5S$ ($[(PhCH_2)Me_3N]^+$ salt): C, 40.04; H, 3.16; Fe, 27.38; S, 3.14. Found: C, 40.15; H, 3.34; Fe, 26.87; S, 3.18. Single crystals of the PPN^+ salt were obtained by slow diffusion of Et_2O into a THF solution of the compound.

Reaction of $[PPN]_2[Fe_3(CO)_9(CCO)]$ with SO_2. On a vacuum line, 2 equiv of SO_2 was added to a 10-mL CH_2Cl_2 solution of 0.1 g of $[PPN]_2[Fe_3(CO)_9(CCO)]$ at −196 °C. After the red-orange solution had been stirred at room temperature, its infrared spectrum showed no bands for the starting cluster and contained a large, broad peak with shoulders from 2010 to 1950 cm^{-1}. The solution was filtered and layered with 15 mL of Et_2O. (The filtration residue gave a bright orange solution when treated with aqueous *o*-phenanthroline; this indicates the presence of Fe^{2+}.) After the layered solvents were allowed to diffuse, about 5 mg of $[PPN]_2[Fe_3(CO)_7(CCO)(SO_2)_2]$ and an orange oil were collected by filtration. A ^{13}C NMR spectrum taken after addition of 1 equiv of SO_2 to an NMR tube containing enriched $[Fe_3(CO)_9(CCO)]^{2-}$ at −78 °C showed at least three cluster species in solution.

X-ray Structure Determinations. Each crystal was mounted quickly in air on a glass fiber with silicon paste and transferred to a cold N_2 stream on a CAD4 diffractometer. The crystal system for $[EtPr_3N]_2[Fe_3(CO)_7(CCO)(SO_2)_2]$ (**1**) was determined to be monoclinic, $P2_1/n$. Although angle β deviates only slightly from 90°, an examination of reflections that are required to be equivalent in an orthorhombic system ruled out this choice. The compound $[PhCH_2Me_3N]_2[Fe_6(CO)_{15}C(SO_2)]$ (**2**) was determined to be orthorhombic with systematic absences consistent with either *Pnma* or $Pna2_1$. The space group ambiguity was resolved as described below. Systematic absences for $[PPN]_2[Fe_5(CO)_{13}C(SO_2)]$ (**3**) indicate the monoclinic space group $P2_1/c$. Data were obtained for **1** in the θ range 2.5–20°. Data collection was prematurely terminated in the 20–25° θ shell because of malfunction of the cold stream. We were unable to obtain another suitable crystal.

The structures were solved with the TEXSAN program package.[23] The iron and sulfur atoms were located by using direct methods (MITHRIL); the other non-hydrogen atomic positions were determined by Fourier techniques. Hydrogen atoms were placed in idealized positions and were included in the structure factor calculation but were not refined. Atoms in the cation were refined isotopically.

During the refinement of **1**, a Fourier map revealed the presence of a large peak (2.4 e/Å^3) located 1.4 Å from the β-carbon of the ethyl chain of an ethyltripropylammonium cation. Large thermal parameters for the terminal carbon of a propyl chain in the same cation indicated a probable disorder of the ethyl and propyl side chains. A carbon atom with a multiplicity of 0.3 was placed at the end of the ethyl chain, and a multiplicity of 0.7 was assigned to the carbon atom in the propyl chain with the large *B* value. These multiplicities were chosen on the basis of trial refinements. Hydrogen atoms were not placed around the disordered atoms. Refinement with this model gave reasonable *B* values for these carbons and resulted in a difference Fourier map whose largest peaks (1.2 e/Å^3 or less) were near the disordered atoms. While this was not a perfect model, use of a more complicated one did not seem warranted considering the quality of the data and the lack of chemical significance of this disorder. The structure was refined to a final value of R_F = 6.6% (R_{wF} = 6.9%) for data with $I > 2\sigma(I)$ with a data to parameter ratio of 8:1 (Tables I and II).

The solution of the structure of **2** was first attempted in the centrosymmetric space group. The cell volume and density indicated $Z = 4$. In the centrosymmetric space group *Pnma*, this constrains the cluster to lie on a mirror plane. The six iron atoms were located, but the position of the sulfur atom was not obvious. Solution of the structure in $Pna2_1$ yielded the positions of the iron and sulfur atoms, and the rest of the atoms were found by Fourier methods. Four iron atoms are coplanar, but mirror symmetry is not preserved by any of the carbonyl ligands. For this reason, refinement in the centrosymmetric space group was not deemed appropriate.

Atoms in the anion of **2** were refined anisotropically. Refinement of the enantiomorph did not give smaller *R* factors, so the originally determined set of coordinates was used in the final refinement. The largest peaks in the final difference map were 1.2 e/Å^3 and were located near the phenyl rings of the cation (Tables I and III).

The crystals of **3** diffracted very weakly, and no significant intensities were observed during a test scan of the range above 2θ = 45°. The Fe, S, and P atoms were refined anisotropically. All H atoms were located from difference Fourier maps and were included as fixed contributors in the refinement. The goodness-of-fit was 2.0. The final difference map was essentially featureless with the highest peak of 0.65 e/Å^3 located near one of the phenyl rings. Final positional parameters are presented in Table IV.

Results and Discussion

Oxidation of Carbide Clusters by SO_2. The butterfly carbide cluster $[Fe_4(CO)_{12}C]^{2-}$ has previously been shown to react with electrophiles to form mononegative clusters that are functionalized at the carbon ligand.[24-26] One possible outcome of the reaction

(20) Hoffmann, R. *J. Phys. Chem.* **1963**, *39*, 1397.
(21) Schilling, B. E. R.; Hoffmann, R. *J. Am. Chem. Soc.* **1979**, *101*, 3456.
(22) Green, M. L. H.; Lucas, C. R. *J. Chem. Soc., Dalton Trans.* **1972**, 1000.
(23) "TEXSAN"; Molecular Structure Corp.: College Station, TX 77843.
(24) Holt, E. M.; Whitmire, K. H.; Shriver, D. F. *J. Am. Chem. Soc.* **1982**, *104*, 5621.
(25) Davis, J. H.; Beno, M. A.; Williams, J. M.; Zimmie, J.; Tachikawa, M.; Muetterties, E. L. *Proc. Natl. Acad. Sci. U.S.A.* **1981**, *78*, 668.

Table I. Crystal Data

compd	1	3	2
formula	$C_{31}H_{52}Fe_3N_2O_{12}S_2$	$C_{86}H_{60}Fe_5N_2O_{15}P_4S$	$C_{36}H_{32}Fe_6N_2O_{17}S$
mol wt	876.00	1736.61	1131.54
cryst dimens, mm	0.39 × 0.23 × 0.20	0.32 × 0.14 × 0.10	0.45 × 0.30 × 0.22
cryst system	monoclinic	monoclinic	orthorhombic
space group	$P2_1/n$	$P2_1/c$	$Pna2_1$
a, Å	10.978 (3)	19.384 (5)	14.642 (2)
b, Å	22.359 (4)	15.644 (6)	15.142 (2)
c, Å	16.810 (3)	26.612 (4)	19.329 (3)
β, deg	90.10 (2)	103.03 (2)	
V, Å^3	4126 (3)	7862 (7)	4285 (2)
Z	4	4	4
μ(Mo Kα), cm^{-1}	12.2	11.0	21.5
radiation	graphite-monochromated Mo Kα (λ = 0.71069 Å)		
2θ range, deg	5–40	4–45	5–50
total no. of data	8766	11240	9066
no. of unique data	5443	10703	6016
no. of unique data with $I > n\sigma(I)$	2516 (n = 2)	5034 (n = 3)	3590 (n = 2)
final no. of variables	335	503	448
R, %	6.6	5.8	4.5
R_w, %	6.9	7.3	4.2
T, °C	−90	−120	−120

Table II. Positional Parameters for $[EtPr_3N]_2[Fe_3(CO)_7(CCO)(SO_2)_2]$ (**1**)

atom	x	y	z
Fe1	0.2775 (2)	0.82353 (8)	0.8231 (1)
Fe2	0.2493 (2)	0.82891 (8)	0.6781 (1)
Fe3	0.2370 (2)	0.92434 (8)	0.7592 (1)
S1	0.2594 (3)	0.9082 (2)	0.8877 (2)
S2	0.2272 (3)	0.9187 (2)	0.6286 (2)
O11	0.0521 (9)	0.7774 (5)	0.8920 (6)
O12	0.4606 (9)	0.7725 (4)	0.9273 (6)
O21	−0.001 (1)	0.7954 (4)	0.6443 (6)
O22	0.3544 (9)	0.7743 (5)	0.5372 (6)
O31	0.346 (1)	1.0432 (5)	0.7573 (5)
O32	−0.021 (1)	0.9538 (5)	0.7694 (6)
O41	0.1513 (8)	0.9162 (4)	0.9381 (5)
O42	0.3697 (9)	0.9329 (4)	0.9253 (5)
O51	0.1104 (8)	0.9338 (4)	0.5914 (4)
O52	0.3325 (8)	0.9434 (4)	0.5856 (5)
O61	0.270 (1)	0.7056 (4)	0.7430 (6)
O99	0.578 (1)	0.9052 (5)	0.7085 (6)
C1	0.373 (1)	0.8658 (6)	0.7470 (7)
C11	0.142 (1)	0.7947 (6)	0.8648 (8)
C12	0.386 (1)	0.7916 (5)	0.8870 (8)
C21	0.099 (1)	0.8090 (6)	0.6568 (8)
C22	0.315 (1)	0.7966 (6)	0.5945 (8)
C31	0.301 (1)	0.9969 (7)	0.7592 (7)
C32	0.080 (1)	0.9429 (6)	0.7662 (8)
C61	0.276 (1)	0.7562 (6)	0.7444 (7)
C99	0.479 (2)	0.8859 (6)	0.7284 (7)

between $[Fe_4(CO)_{12}C]^{2-}$ and sulfur dioxide might have produced a compound containing a sulfur–carbon bond. Instead, the product of this reaction is a triiron ketenylidene species (eq 1). The 80%

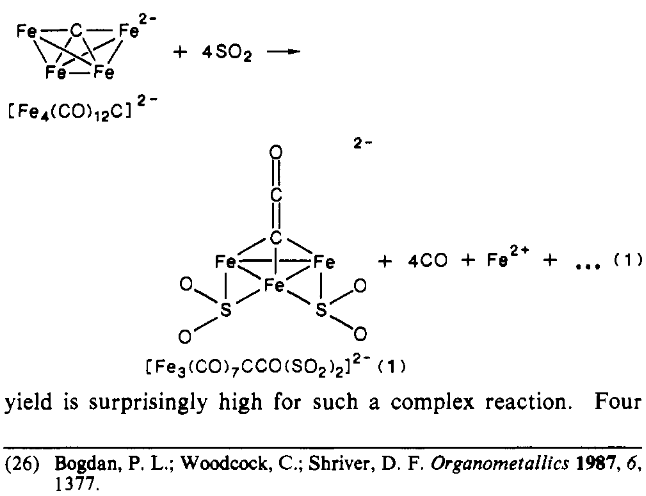

yield is surprisingly high for such a complex reaction. Four equivalents of SO_2 is required to take the reaction to completion. The fate of the sulfur dioxide that is not incorporated into the cluster is uncertain; some CH_2Cl_2-insoluble residue was removed at the end of the reaction but could not be identified by vibrational spectroscopy or spot qualitative analysis. Formation of a sulfur-containing oxyanion can be postulated to balance the redox reaction.

An ORTEP drawing of **1**, shown in Figure 1, consists of a triangle of iron atoms, bridged on two edges by sulfur dioxide ligands and

Table III. Positional Parameters for $[(PhCH_2)Me_3N]_2[Fe_6(CO)_{15}C(SO_2)]$ (**2**)

	x	y	z
Fe1	0.0061 (1)	0.4912 (1)	0.9840
Fe2	−0.01546 (7)	0.60812 (7)	1.0799 (1)
Fe3	0.14001 (7)	0.51188 (7)	1.0780 (1)
Fe4	0.02123 (8)	0.4843 (1)	1.17829 (8)
Fe5	−0.11401 (7)	0.45960 (7)	1.0842 (1)
Fe6	0.03832 (7)	0.36448 (7)	1.0769 (1)
S1	0.1655 (1)	0.5192 (2)	1.1887 (1)
O11	0.1528 (5)	0.5356 (5)	0.8886 (4)
O12	−0.1265 (5)	0.4512 (5)	0.8754 (4)
O21	0.1038 (4)	0.7623 (4)	1.0862 (5)
O22	−0.0527 (4)	0.6752 (4)	0.9424 (4)
O23	−0.1581 (5)	0.7138 (4)	1.1432 (4)
O31	0.2856 (5)	0.3955 (5)	1.0314 (4)
O32	0.2619 (5)	0.6518 (5)	1.0315 (4)
O41	0.0287 (5)	0.3348 (5)	1.2739 (4)
O42	−0.0466 (5)	0.6193 (5)	1.2740 (4)
O51	−0.2617 (4)	0.5776 (4)	1.0419 (4)
O52	−0.2075 (5)	0.3207 (5)	1.0055 (4)
O53	−0.1933 (4)	0.4279 (5)	1.2198 (4)
O61	0.0683 (5)	0.3005 (4)	0.9354 (4)
O62	−0.0772 (5)	0.2207 (5)	1.1235 (5)
O63	0.1864 (5)	0.2557 (5)	1.1339 (4)
O71	0.2254 (4)	0.4514 (5)	1.2166 (4)
O72	0.1850 (4)	0.6066 (5)	1.2155 (4)
C1	0.0135 (5)	0.4874 (5)	1.0807 (7)
C11	0.0967 (6)	0.5174 (6)	0.9277 (4)
C12	−0.0754 (7)	0.4656 (6)	0.9177 (5)
C21	0.0594 (5)	0.6995 (6)	1.0876 (6)
C22	−0.0348 (6)	0.6247 (6)	0.9854 (5)
C23	−0.1035 (7)	0.6715 (6)	1.1176 (5)
C31	0.2267 (6)	0.4381 (6)	1.0505 (5)
C32	0.2111 (6)	0.5991 (7)	1.0514 (5)
C41	0.0251 (6)	0.3939 (6)	1.2362 (5)
C42	−0.0194 (6)	0.5682 (6)	1.2362 (5)
C51	−0.2015 (6)	0.5350 (6)	1.0591 (5)
C52	−0.1696 (6)	0.3740 (6)	1.0368 (5)
C53	−0.1525 (6)	0.4407 (6)	1.1705 (5)
C61	0.0511 (6)	0.3413 (6)	0.9852 (5)
C62	−0.0348 (6)	0.2792 (6)	1.1037 (5)
C63	0.1315 (6)	0.3021 (6)	1.1102 (5)

(26) Bogdan, P. L.; Woodcock, C.; Shriver, D. F. *Organometallics* **1987**, *6*, 1377.

Table IV. Positional Parameters for $[PPN]_2[Fe_5(CO)_{13}C(SO_2)]$ (3)

atom	x	y	z
Fe1	0.83893 (7)	0.2694 (1)	0.05351 (6)
Fe2	0.71746 (7)	0.1908 (1)	0.00683 (6)
Fe3	0.73831 (8)	0.3386 (1)	−0.02694 (6)
Fe4	0.85787 (8)	0.2871 (1)	−0.03895 (6)
Fe5	0.83909 (8)	0.1330 (1)	−0.00212 (6)
S	0.6507 (1)	0.3021 (2)	−0.0003 (1)
O1	0.5806 (4)	0.2984 (5)	−0.0409 (3)
O2	0.6489 (3)	0.3421 (5)	0.0495 (3)
O11	0.8330 (4)	0.1720 (5)	0.1458 (3)
O12	0.9926 (4)	0.2782 (5)	0.0959 (3)
O13	0.8104 (4)	0.4266 (6)	0.1013 (3)
O21	0.6752 (4)	0.0984 (5)	0.0873 (3)
O22	0.6269 (4)	0.0904 (5)	−0.0806 (3)
O31	0.6560 (4)	0.3424 (6)	−0.1381 (3)
O32	0.7353 (4)	0.5217 (6)	−0.0077 (3)
O41	0.8106 (5)	0.2356 (7)	−0.1499 (4)
O42	1.0119 (4)	0.2885 (6)	−0.0157 (3)
O43	0.8527 (4)	0.4691 (6)	−0.0606 (3)
O51	0.7925 (5)	0.0271 (7)	−0.0968 (4)
O52	0.8067 (4)	0.0087 (6)	0.0673 (3)
O53	0.9908 (4)	0.0945 (6)	0.0280 (3)
C1	0.7868 (5)	0.2332 (7)	−0.0188 (4)
C11	0.8312 (5)	0.2085 (7)	0.1068 (4)
C12	0.9313 (6)	0.2756 (8)	0.0763 (4)
C13	0.8190 (6)	0.3680 (8)	0.0776 (4)
C21	0.6924 (5)	0.1354 (7)	0.0566 (4)
C22	0.6623 (5)	0.1318 (7)	−0.0451 (4)
C31	0.6888 (6)	0.3430 (9)	−0.0937 (5)
C32	0.7370 (6)	0.4497 (8)	−0.0141 (4)
C41	0.8337 (7)	0.256 (1)	−0.1035 (5)
C42	0.9516 (6)	0.2835 (8)	−0.0249 (4)
C43	0.8508 (6)	0.3986 (9)	−0.0489 (5)
C51	0.8121 (6)	0.0721 (9)	−0.0594 (5)
C52	0.8180 (5)	0.0602 (8)	0.0414 (4)
C53	0.9309 (6)	0.1106 (8)	0.0161 (4)

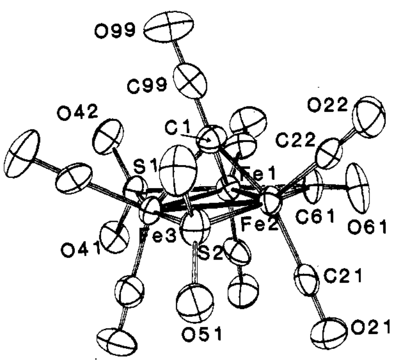

Figure 1. ORTEP drawing of the $[Fe_3(CO)_7(CCO)(SO_2)_2]^{2-}$ anion. Ellipsoids are drawn at the 50% probability level.

on the other by a carbonyl ligand. The Fe–Fe distances bridged by SO_2 ligands are similar to those found in $[Fe_3(CO)_9(CCO)]^{2-}$, 2.534 (3) versus 2.564 (4) Å,[16] while the CO-bridged edge is quite short, 2.459 (3) Å. The geometry about the sulfur is distorted tetrahedral. In comparison with the geometry of the dimeric S-bridged iron compounds $Fe_2(CO)_8(SO_2)$ (Fe–Fe = 2.717 (4) Å; Fe–S = 2.220 (5) Å; Fe–S–Fe = 75.6°)[27] and $[CpFeCO]_2(CO)(SO_2)$ (Fe–Fe = 2.590 (1) Å; Fe–S = 2.178 (1) Å; Fe–S–Fe = 72.96 (3)° (average for two discrete molecules)),[28] the Fe–S distances are about the same (2.190 (4), 2.203 (4) Å), but the SO_2-bridged Fe–Fe distances observed here are shorter (2.534 (3) Å), resulting in smaller Fe–S–Fe angles (70.5 (1), 70.6 (1)°). The ketenylidene CCO ligand is essentially linear and tilted 13° from a perpendicular to the face defined by the three iron atoms. This is in contrast to the 33° tilt of the CCO observed for $[Fe_3(CO)_9(CCO)]^{2-}$. The general disposition of ligands in **1** is

Table V. Bond Distances (Å) and Angles (deg) for $[EtPr_3N]_2[Fe_3(CO)_7(CCO)(SO_2)_2]$ (1)

Fe1–Fe2	2.459 (2)	S2–O51	1.471 (9)
Fe2–Fe3	2.534 (3)	S2–O52	1.465 (8)
Fe3–Fe1	2.534 (2)	C1–C99	1.30 (2)
Fe1–S1	2.192 (4)	C99–O99	1.22 (2)
Fe3–S1	2.203 (4)	Fe1–C11	1.77 (1)
Fe2–S2	2.187 (4)	Fe1–C12	1.75 (2)
Fe3–S2	2.201 (4)	Fe1–C61	2.00 (1)
Fe1–C1	1.90 (1)	Fe2–C21	1.75 (2)
Fe2–C1	1.96 (1)	Fe2–C22	1.74 (1)
Fe3–C1	1.99 (1)	Fe2–C61	1.99 (1)
S1–O41	1.470 (8)	Fe3–C31	1.77 (2)
S1–O42	1.472 (9)	Fe3–C32	1.78 (2)
Fe1–Fe2–Fe3	60.97 (7)	Fe1–C1–Fe2	79.0 (5)
Fe2–Fe1–Fe3	60.96 (7)	Fe1–C1–Fe3	81.2 (5)
Fe1–Fe3–Fe2	58.07 (7)	Fe2–C1–Fe3	79.7 (5)
Fe1–S1–Fe3	70.4 (1)	O41–S1–O42	111.8 (5)
Fe2–S2–Fe3	70.5 (1)	O51–S2–O52	113.1 (5)
Fe1–C1–C99	146 (1)	C1–C99–O99	178 (1)
Fe2–C1–C99	129 (1)	Fe1–C61–O61	140 (1)
Fe3–C1–C99	118 (1)	Fe1–C61–O61	143 (1)

nearly identical with that observed in $[Ru_3(CO)_9(CCO)]^{2-}$,[29] where the metal triangle is bridged by three CO's as opposed to one CO and two SO_2's.

The ^{13}C NMR spectrum of $[Fe_3(CO)_7(CCO)(SO_2)_2]^{2-}$ can be assigned in accord with the solid-state structure. The α-carbon of the ketenylidene ligand (*C*CO) resonates at high field, δ 6.6, and the β-carbon (C*C*O) appears at δ 167.4. These shifts are similar to those observed for M_3-coordinated CCO ligands, in $[Fe_3(CO)_9(CCO)]^{2-}$ (α-C, δ 95.3; β-C, δ 179.8),[16] $[Ru_3(CO)_9(CCO)]^{2-}$ (α-C, δ −28.3; β-C, +159.1),[29] and $[Os_3(CO)_9(CCO)]^{2-}$ (α-C, δ 31.2; β-C, δ 168.3).[30] The upfield position of the α-carbon signal for $[Fe_3(CO)_7(CCO)(SO_2)_2]^{2-}$ and $[Ru_3(CO)_9(CCO)]^{2-}$ may be related to their similar carbonyl dispositions. In contrast, $[Fe_3(CO)_9(CCO)]^{2-}$ and $[Os_3(CO)_9(CCO)]^{2-}$ possess all terminal carbonyl ligands in axial and equatorial positions. Weak satellites (about 89 Hz) on the δ 167.4 peak are observed for the C–C coupling for the sulfur dioxide substituted cluster. The terminal carbonyls on $[Fe_3(CO)_7(CCO)(SO_2)_2]^{2-}$ show a 1:2:2:1 pattern at all temperatures, and the bridging carbonyl peak appears at δ 257. The bridging carbonyl ligand absorption in the solution infrared spectrum appears at 1810 cm^{-1}. The CO stretching frequencies in solution and the solid state are shifted by about 40 cm^{-1} to higher energy than those of $[Fe_3(CO)_9(CCO)]^{2-}$ and along with the upfield shift of the carbonyl resonances in the ^{13}C NMR spectrum (ca. 10 ppm) indicate that the sulfur dioxide ligands are functioning as electron acceptors.

It seemed likely that SO_2 substitution on the triiron ketenylidene cluster would yield the same product; however, reaction of $[Fe_3(CO)_9(CCO)]^{2-}$ with 2 mol of SO_2 gives only a 5% yield of $[Fe_3(CO)_7(CCO)(SO_2)_2]^{2-}$, a large amount of Fe^{2+}, and other cluster products (eq 2). Thus the triiron ketenylidene cluster

$$[Fe_3(CO)_9(CCO)]^{2-} + 2SO_2 \rightarrow [Fe_3(CO)_7(CCO)(SO_2)_2]^{2-} + Fe^{2+} + ... + \text{other cluster products} \quad (2)$$

appears too strong a reducing agent toward SO_2. Even the addition of 1 equiv of SO_2 to a methylene chloride solution of $[PPN]_2[Fe_3(CO)_9(CCO)]$ in an NMR tube at −78 °C produces a ^{13}C NMR spectrum with resonances suggestive of the presence of several cluster products.

The sulfur dioxide substituted ketenylidene cluster is reactive toward both electrophiles (H^+ and CH_3^+) and nucleophiles (CH_3Li), though the products were too unstable to isolate. Attempts to follow the protonation of **1** by NMR spectroscopy at low temperatures were also unsuccessful. The cluster decomposes in methanol solution over the period of 1 h,[31] but no new carbonyl

(27) Meunier-Piret, J.; Piret, P.; VanMeerssche, M. *Bull. Soc. Chim. Belg.* **1967**, *76*, 374.
(28) Churchill, M. R.; Kalra, K. L. *Inorg. Chem.* **1973**, *12*, 1650.
(29) Sailor, M. J.; Shriver, D. F. *Organometallics* **1985**, *4*, 1476.
(30) Went, M. J.; Sailor, M. J.; Bogdan, P. L.; Brock, C. P.; Shriver, D. F. *J. Am. Chem. Soc.* **1987**, *109*, 6023.

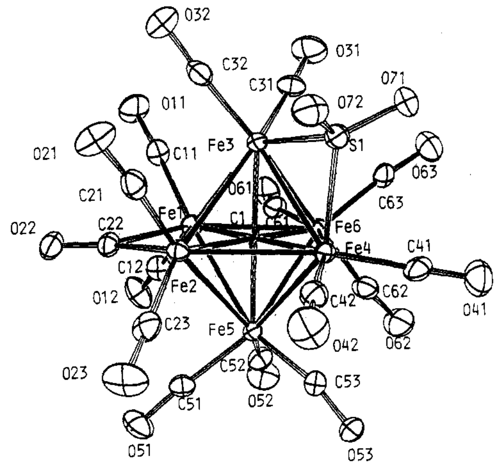

Figure 2. ORTEP drawing of the $[Fe_6(CO)_{15}C(SO_2)]^{2-}$ anion. Ellipsoids are drawn at the 50% probability level.

stretches are observed as the bands from starting material decrease in intensity.

Substitution of SO_2 on Carbido Carbonyl Clusters. When $[PPN]_2[Fe_6(CO)_{16}C]$ reacts with sulfur dioxide at room temperature, a clean substitution of SO_2 for one CO ligand occurs, as judged by *PVT* measurement of gaseous reactants and products on a vacuum line (eq 3). Salts of $[Fe_6(CO)_{16}C]^{2-}$ with other

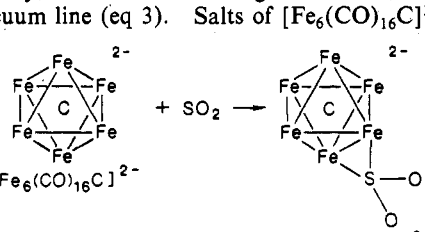

$[Fe_6(CO)_{16}C]^{2-}$ + SO_2 → + CO (3)

$[Fe_6(CO)_{15}C(SO_2)]^{2-}$ (**2**)

cations react more slowly with SO_2 and require excess reagent to go to completion. This effect may be due either to cation–anion interaction or to solvent effects, because coordinating solvents must be employed to solubilize alkylammonium or alkali-metal salts of the starting material.

Spectra of **2** are very similar to those of the starting material. The infrared CO stretching frequencies are shifted slightly to higher energy and the terminal carbonyl ^{13}C NMR resonances are shifted to higher field, again indicating the electron-accepting character of SO_2 relative to CO. The NMR spectrum of the carbonyl region contains a single peak for $[Fe_6(CO)_{15}C(SO_2)]^{2-}$ from −90 °C to room temperature, analogous to $[Fe_6(CO)_{16}C]^{2-}$. Upon further cooling, the terminal and bridging carbonyls are observable at about −130 °C, but loss of resolution prevented the determination of relative intensities. The mull infrared spectrum contains a bridging CO absorption at 1777 cm^{-1} and an Fe–C stretch for the interstitial carbon at 806 cm^{-1}.

A single-crystal X-ray diffraction study confirmed the identity of the cluster as a simple monosubstitution product. An ORTEP drawing of the benzyltrimethylammonium salt of $[Fe_6(CO)_{15}C(SO_2)]^{2-}$ is shown in Figure 2. The octahedral array of iron atoms with an interstitial carbide ligand is essentially identical with that of the parent compound $[Fe_6(CO)_{16}C]^{2-}$; both show a range of Fe–Fe distances. For **2**, the range is from 2.582 (2) to 2.723 (2) Å. The Me_4N^+ salt of $[Fe_6(CO)_{16}C]^{2-}$ contains three semibridging carbonyls, and the carbide ligand is slightly displaced from the center of the octahedron.[32] In compound **2** there is an edge-bridging sulfur dioxide, two semibridging carbonyls, and one

Table VI. Bond Distances (Å) and Angles (deg) for $[PhCH_2)Me_3N]_2[Fe_6(CO)_{15}C(SO)_2]$ (**2**)

Fe1–Fe2	2.582 (2)	Fe5–Fe6	2.659 (2)
Fe1–Fe3	2.691 (2)	Fe3–S1	2.174 (3)
Fe1–Fe5	2.659 (2)	Fe4–S1	2.186 (3)
Fe1–Fe6	2.670 (2)	Fe1–C1	1.87 (1)
Fe2–Fe3	2.703 (2)	Fe2–C1	1.877 (7)
Fe2–Fe4	2.723 (2)	Fe3–C1	1.890 (7)
Fe2–Fe5	2.673 (2)	Fe4–C1	1.89 (1)
Fe3–Fe4	2.637 (2)	Fe5–C1	1.915 (7)
Fe3–Fe6	2.683 (2)	Fe6–C1	1.898 (7)
Fe4–Fe6	2.682 (2)	S1–O71	1.454 (7)
Fe4–Fe5	2.714 (2)	S1–O72	1.451 (7)
Fe1–Fe2–Fe4	90.31 (5)	O72–S1–O71	113.0 (4)
Fe2–Fe1–Fe6	91.80 (7)	Fe1–C1–Fe2	87.1 (4)
Fe5–Fe1–Fe3	90.65 (6)	Fe1–C1–Fe3	91.4 (5)
Fe5–Fe2–Fe3	90.09 (5)	Fe1–C1–Fe6	90.2 (5)
Fe4–Fe3–Fe1	89.83 (5)	Fe1–C1–Fe5	89.2 (5)
Fe6–Fe3–Fe2	88.92 (5)	Fe4–C1–Fe3	88.5 (5)
Fe6–Fe4–Fe2	88.53 (7)	Fe4–C1–Fe2	92.5 (5)
Fe3–Fe4–Fe5	90.60 (7)	Fe4–C1–Fe5	91.0 (4)
Fe1–Fe5–Fe4	88.89 (5)	Fe4–C1–Fe6	90.1 (4)
Fe6–Fe5–Fe2	90.07 (5)	Fe1–C22–O22	133.4 (8)
Fe5–Fe6–Fe3	90.83 (5)	Fe2–C22–O22	145.6 (8)
Fe1–Fe6–Fe4	89.32 (5)	Fe5–C53–O53	166.8 (8)
Fe3–S1–Fe4	74.45 (9)	Fe6–C61–O61	157.8 (9)

symmetrically bridging carbonyl ligand. The central carbide atom is equidistant from all six irons within 3σ error limits. The S-bridged Fe–Fe distance (2.637 (2) Å), Fe–S distances (2.174, 2.186 (3) Å), and Fe–S–Fe angle (74.45 (8)°) are all similar to those found in dinuclear iron compounds with SO_2 bridges.[27,28]

In contrast to the triiron sulfur dioxide cluster **1**, the hexairon cluster $[Fe_6(CO)_{15}C(SO_2)]^{2-}$ is remarkably stable. For example, it is air-stable in solution and unreactive at acetone reflux temperature. When heated to 200 °C under vacuum, $[Fe_6(CO)_{15}C(SO_2)]^{2-}$ liberates SO_2, CO, and CO_2 and regenerates some $[Fe_6(CO)_{16}C]^{2-}$. Protonation with excess CF_3SO_3H leads to formation of a mononegative cluster having no SO_2 stretching bands in the IR. This cluster has not yet been characterized. Oxidation of **2** with Ag^+ or $C_7H_7^+$ gives more than one product; mass spectral evidence suggests the presence of $Fe_5(CO)_{15}C$ along with other neutral clusters, which may be formulated as $Fe_6(CO)_{16}CS$ and $Fe_5(CO)_{13}CS$.

Reaction of the $[Fe_2(CO)_{14}C]^{2-}$ Anion with SO_2. In the series of anionic carbido carbonyls Fe_3–Fe_6, the alkylation reactivity observed for the five- and six-metal clusters differs from that of the three- and four-metal clusters. The lower nuclearity compounds are alkylated at the metal-bound carbon atom, whereas the site of reactivity for the larger clusters is a carbonyl oxygen.[24,33] The chemistry of $[Fe_5(CO)_{14}C]^{2-}$ is also similar to that of $[Fe_4(CO)_{12}C]^{2-}$, for these are the only two members of the series for which the neutral carbido carbonyls are stable.[25,34] It was of interest then to determine whether the reaction of the pentairon carbide cluster with SO_2 would result in substitution or oxidation.

The pentairon carbide anion of $[PPN]_2[Fe_5(CO)_{14}C]$ reacts with 1 mol of SO_2 according to eq 4. However, a higher yield

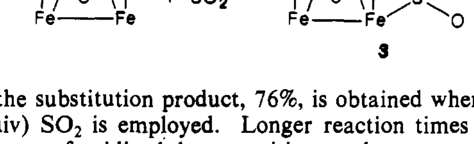

+ SO_2 → + CO (4)

3

of the substitution product, 76%, is obtained when excess (2.8 equiv) SO_2 is employed. Longer reaction times increase the amount of oxidized decomposition products.

The asymmetric S–O stretch is at 1028 cm^{-1}. There are no low-frequency infrared bands characteristic of bridging carbonyls

(31) Cluster-bound CCO ligands are known to react with MeOH: (a) Sievert, A. C.; Strickland, D. S.; Shapley, J. R.; Steinmetz, G. R.; Geoffroy, G. L. *Organometallics* **1982**, *1*, 214. (b) Holmgren, J. S.; Shapley, J. R. *Organometallics* **1984**, *3*, 1322. (c) Seyferth, D.; Hallgren, J. E.; Eschbach, C. S. *J. Am. Chem. Soc.* **1974**, *96*, 1730.

(32) Churchill, M. R.; Wormald, J. *J. Chem. Soc., Dalton Trans.* **1974**, 2410.

(33) Kolis, J. W.; Basolo, F.; Shriver, D. F. *J. Am. Chem. Soc.* **1982**, *104*, 5626.

(34) Jeannin, Y.; Gourdon, A. *J. Organomet. Chem.* **1985**, *290*, 199.

Table VII. Selected Bond Lengths (Å) and Angles (deg) for $[PPN]_2[Fe_5(CO)_{13}C(SO_2)]$ (3)

Fe1-Fe2	2.641 (2)	Fe2-C22	1.73 (1)
Fe1-Fe3	2.643 (2)	Fe3-S	2.170 (3)
Fe1-Fe4	2.624 (2)	Fe3-C1	1.89 (1)
Fe1-Fe5	2.597 (2)	Fe3-C31	1.73 (1)
Fe2-Fe3	2.564 (2)	Fe3-C32	1.77 (1)
Fe2-Fe5	2.676 (2)	Fe4-C1	1.87 (1)
Fe3-Fe4	2.638 (2)	Fe4-C41	1.70 (1)
Fe4-Fe5	2.674 (2)	Fe4-C42	1.79 (1)
Fe1-C1	1.95 (1)	Fe4-C43	1.76 (1)
Fe1-C11	1.76 (1)	Fe5-C1	1.86 (1)
Fe1-C12	1.75 (1)	Fe5-C51	1.73 (1)
Fe1-C13	1.77 (1)	Fe5-C52	1.77 (1)
Fe2-S	2.164 (3)	Fe5-C53	1.77 (1)
Fe2-C1	1.86 (1)	S-O1	1.464 (8)
Fe2-C21	1.79 (1)	S-O2	1.476 (7)

Fe2-Fe1-Fe4	90.01 (7)	Fe1-C1-Fe4	86.6 (4)
Fe3-Fe1-Fe5	90.99 (7)	Fe1-C1-Fe5	86.1 (4)
Fe3-Fe2-Fe5	90.97 (7)	Fe2-C1-Fe3	86.4 (4)
Fe2-Fe3-Fe4	91.38 (7)	Fe2-C1-Fe4	173.0 (6)
Fe3-Fe4-Fe5	89.42 (7)	Fe2-C1-Fe5	92.3 (5)
O1-S-O2	112.4 (4)	Fe3-C1-Fe4	89.0 (5)
Fe2-S-Fe3	72.6 (1)	Fe3-C1-Fe5	173.0 (6)
Fe1-C1-Fe2	87.9 (4)	Fe4-C1-Fe5	91.6 (4)
Fe1-C1-Fe3	87.0 (4)		

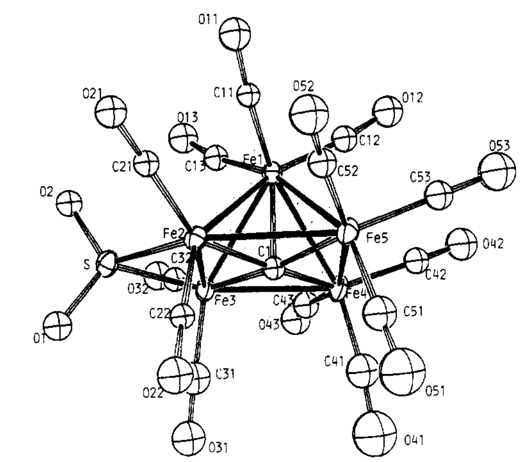

Figure 3. ORTEP drawing of the $[Fe_5(CO)_{13}C(SO_2)]^{2-}$ anion. Ellipsoids are drawn at 50% probability level.

in the solution or mull spectra. The major CO stretch appears at 1981 cm^{-1} in solution as compared with 1955 cm^{-1} for $[Fe_5(CO)_{14}C]^{2-}$. The shape and positions of the IR bands at 817 and 793 cm^{-1} are suggestive of iron–carbon stretching modes in a five-metal square-pyramidal structure.[35] A ^{13}C NMR spectrum indicates the existence of four types of terminal CO environments in the region δ 220–212 and the carbide resonance at δ 475.

The formulation of this compound as a pentairon carbide cluster was confirmed by a single-crystal X-ray structure determination, which shows that the SO_2 bridges the basal iron atoms (Figure 3). The five iron atoms are in a square-pyramidal array with the carbide ligand residing in the basal face. All of the carbonyl ligands are in terminal positions, consistent with the spectroscopic data. The Fe–Fe distances are similar to those observed in $Fe_5(CO)_{15}C$ and $[Bu_4N]_2[Fe_5(CO)_{14}C]$,[34] although the difference between the Fe(apical)–Fe(basal) and between the Fe(basal)–Fe(basal) is much less pronounced in 3 than in $[Fe_5(CO)_{14}C]^{2-}$. The shortest Fe–Fe distance (2.564 (2) Å) occurs for the iron atoms bridged by SO_2. The apical iron atom Fe1–carbide C1 atom distance is 1.95 (1) Å and is significantly longer than the equatorial Fe–C1 distances (1.86–1.89 Å). The carbide atom is 0.10 Å below the least-squares plane through the Fe2Fe3Fe4Fe5 atoms. The

(35) Oxton, I. A.; Powell, D. B.; Goudsmit, R. J.; Johnson, B. F. G.; Lewis, J.; Nelson, W. J. H.; Nichols, J. N.; Rosales, M. J.; Vargas, M. D.; Whitmire, K. H. *Inorg. Chim. Acta* **1982**, *64*, L259.

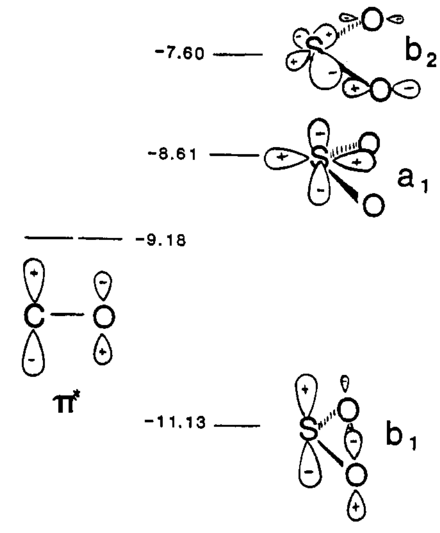

Figure 4. Energy-level diagram for lowest unoccupied molecular orbitals of CO and SO_2, calculated by the extended Hückel method. The energies are in electronvolts.

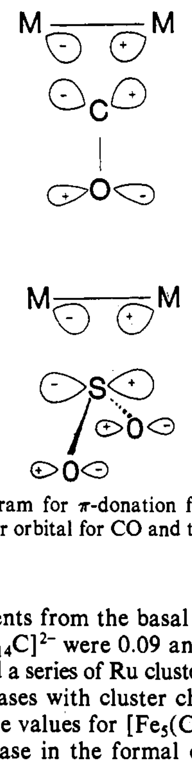

Figure 5. Orbital diagram for π-donation from a filled metal-based orbital to the 5σ acceptor orbital for CO and the $3b_1$ acceptor orbital of SO_2.

analogous displacements from the basal plane found in $Fe_5(CO)_{15}C$ and $[Fe_5(CO)_{14}C]^{2-}$ were 0.09 and 0.18 Å, respectively. For the Fe clusters and a series of Ru clusters,[36] the deviation from the basal plane increases with cluster charge. The significant difference between the values for $[Fe_5(CO)_{14}C]^{2-}$ and 3 can be explained by a decrease in the formal charge caused by SO_2 substitution.

Comparison of Cluster-Bound SO_2 and CO. Carbon monoxide and sulfur dioxide may serve as both σ-electron donors and π-electron acceptors toward metal centers. The primary differences in their molecular orbital descriptions involve the charges and electron acceptor orbitals of the free molecules.[1,2,5,14] In contrast to CO, the S atom in SO_2 carries a significant positive charge. Free SO_2 has a surprisingly high electron affinity of 1.1 eV.[37] Two degenerate orbitals (π^*) are available in the CO ligand for π-back-bonding, whereas SO_2 has three acceptor orbitals, one of lower energy than those of CO (b_1) and two of higher energy (b_2 and a_1) (Figure 4). b_1 is the most important electron acceptor orbital for SO_2 and has the same π-symmetry as the degenerate CO orbitals. The favorable interaction of bridging CO and SO_2

(36) Johnson, B. F. G.; Lewis, J.; Nicholls, J. N.; Puga, J.; Raithby, P. R.; McPartlin, M.; Clegg, W. *J. Chem. Soc., Dalton Trans.* **1983**, 277.

(37) Janousek, B. K.; Brauman, J. I. In *Gas Phase Ion Chemistry*; Bowers, M. T., Ed.; Academic: New York, 1979; Vol. 2, Chapter 10, p 53.

Table VIII. Calculated Atomic Charges for Iron Atoms and CCO Ligands

atom	$[Fe_3(CO)_9(CCO)]^{2-}$	$[Fe_3(CO)_6(\mu\text{-}CO)_3(CCO)]^{2-}$	$[Fe_3(CO)_7(CCO)(SO_2)_2]^{2-}$
Fe1	+0.11	+0.13	+0.40
Fe2	+0.25	+0.24	+0.50
Fe3	+0.11	+0.13	+0.54
C_α	−0.52	−0.50	−0.43
C_β	+0.77	+0.81	+0.85
O	−1.00	−0.99	−0.98

Table IX. Cyclic Voltammetric Peak Voltages for First Oxidation and Reduction Waves[a]

cluster	E_p, V	
	anodic	cathodic
$[Fe_6(CO)_{16}C]^{2-}$	+0.59[d]	−1.32
$[Fe_6(CO)_{15}C(SO_2)]^{2-}$	+0.84	−1.01
$[Fe_5(CO)_{14}C]^{2-}$[b]	+0.45[d]	−1.38
$[Fe_5(CO)_{13}C(SO_2)]^{2-}$	+0.72	−1.19[d]
$[Fe_3(CO)_9(CCO)]^{2-}$	+0.12[d]	<−1.95[c]
$[Fe_3(CO)_7(CCO)(SO_2)_2]^{2-}$	+0.77	−1.85

[a] Measured in CH_3CN with Bu_4NBF_4 as supporting electrolyte at 100 mV/s scan rate, referenced to Ag wire. [b] Reference 34. Values corrected to Ag. [c] The cluster reduction cannot be observed before the reduction of the PPN^+ cation at −1.95 V. [d] Denotes part of a reversible couple.

ligands with two metal centers is illustrated in Figure 5.

To compare the bonding of μ-SO_2 and CO, an extended Hückel molecular orbital calculation was carried out on the $[Fe_3(CO)_7(CCO)(SO_2)_2]^{2-}$ anion and compared with previous calculations on $[Fe_3(CO)_9(CCO)]^{2-}$.[38] In order to compare bridging SO_2 and bridging CO, two ligand dispositions on $[Fe_3(CO)_9(CCO)]^{2-}$ were considered, one in which the carbonyls are axial and equatorial (the structure as determined by X-ray crystallography) and a second in which there are three bridging carbonyls around the iron triangle. The latter is analogous to a known ruthenium cluster.[29]

The frontier orbitals are similar in all three calculations. There are no significant changes in atomic contributions or energies in the HOMO's and LUMO's among the orbitals calculated for the three clusters. The frontier orbitals in all cases are primarily metal and ketenylidene based and are composed of three energetically similar orbitals on each side of the HOMO–LUMO gap. The sulfur atoms contribute to one of the unoccupied orbitals. The HOMO–LUMO energy separations are as follows: $[Fe_3(CO)_9(CCO)]^{2-}$, 1.7 eV; $[Fe_3(CO)_6(\mu\text{-}CO)_3(CCO)]^{2-}$, 2.2 eV; $[Fe_3(CO)_7(SO_2)_2(CCO)]^{2-}$, 2.3 eV.[39]

An interesting difference in the results for these compounds is found in the calculated net atomic charges. The values for the iron atoms and CCO ligand in the three calculations are given in Table VIII. The iron atoms are significantly more positive in the sulfur dioxide substituted cluster. Introduction of bridging CO ligands into $[Fe_3(CO)_9(CCO)]^{2-}$ does not significantly affect the calculated iron atom charges. Considerable negative charge is delocalized onto the four sulfur-bound oxygen atoms, as well as on the carbonyl oxygen atoms.

(38) Went, M. J., Northwestern University, unpublished results, 1985.
(39) Energies calculated for HOMO and LUMO: $[Fe_3(CO)_9(CCO)]^{2-}$, −11.09 and −9.43 eV; $[Fe_3(CO)_6(\mu\text{-}CO)_3(CCO)]^{2-}$, −11.52 and −9.31 eV; $[Fe_3(CO)_7(CCO)(SO_2)_2]^{2-}$, −11.85 and −9.58 eV.

Table X. IR and NMR Spectroscopic Data

compd	ν(CO), cm^{-1} [a]	^{13}C δ(CO)[b]
$[Fe_3(CO)_9(CCO)]^{2-}$[c]	1932[c]	222[c]
$[Fe_3(CO)_7(CCO)(SO_2)_2]^{2-}$	1985	211
$[Fe_5(CO)_{14}C]^{2-}$	1955	227
$[Fe_5(CO)_{13}C(SO_2)]^{2-}$	1981	219
$[Fe_6(CO)_{16}C]^{2-}$	1961	228
$[Fe_6(CO)_{15}C(SO_2)]^{2-}$	1982	221

[a] Major CO stretch for PPN^+ salts in CH_2Cl_2 solution. [b] Average value for PPN^+ salts measured in 20% CD_2Cl_2. [c] Data from ref 16.

As another measure of the electronic effect of SO_2 ligands on the iron carbido carbonyl clusters, the potentials for the first oxidation and reduction waves of these clusters were determined by cyclic voltammetry (Table IX). The oxidations are electrochemically irreversible for the sulfur dioxide containing clusters and reversible for the carbonyl clusters. Only $[Fe_5(CO)_{13}C(SO_2)]^{2-}$ is reversibly reduced on the CV time scale. In agreement with the above discussion, the clusters containing sulfur dioxide are uniformly more difficult to oxidize and easier to reduce than the parent carbido carbonyls. For the substitution of one carbonyl, this shift is on the order of 0.20–0.30 V; substitution of two sulfur dioxide ligands onto the cluster increases the observed shift to 0.65 V.

For the triiron clusters, the calculated difference in their HOMO energies is 0.76 V, which compares reasonably well to the 0.65 V difference observed in their oxidation potentials. The HOMO and LUMO of $[Fe_3(CO)_7(CCO)(SO_2)_2]^{2-}$ are both stabilized relative to those of $[Fe_3(CO)_9(CCO)]^{2-}$.[39] These results of the extended Hückel calculations are consistent with the trend toward more difficult oxidation and easier reduction for the sulfur dioxide substituted clusters.

The differences in the anodic peak potentials, shifts in CO stretching frequencies, and changes in ^{13}C NMR chemical shifts (Table X) can all be correlated with the sulfur dioxide to metal ratio present in the cluster. These data suggest that the sulfur dioxide ligand on these clusters is strongly electron accepting.

Acknowledgment. This research was funded by the NSF Synthetic Inorganic Organometallic Chemistry Program. P.L.B. thanks the NSF for an NSF Predoctoral Fellowship and M. J. Went for some extended Hückel calculations.

Registry No. $[PPN]_2[Fe_3(CO)_7(CCO)(SO_2)_2]$, 114220-91-6; $[PPN]_2[Fe_6(CO)_{15}C(SO_2)]$, 114220-96-1; $[EtPr_3N][Fe_3(CO)_7(CCO)(SO_2)_2]$, 114249-67-1; $[(PhCH_2)Me_3N][Fe_6(CO)_{15}C(SO_2)]$, 114220-95-0; $[PPN]_2[Fe_5(CO)_{13}C(SO_2)]$, 114249-69-3; $[PPN]_2[Fe_4(CO)_{12}C]$, 74792-05-5; $[EtPr_3N][Fe_4(CO)_{12}C]$, 114220-93-8; $[PPN]_2[Fe_6(CO)_{16}C]$, 78568-53-3; $[(PhCH_2)Me_3N][Fe_6(CO)_{16}C]$, 114220-92-7; $[PPN]_2[Fe_5(CO)_{14}C]$, 84786-39-0; $[PPN]_2[Fe_3(CO)_9(CCO)]$, 87710-96-1; CO, 630-08-0; SO_2, 7446-09-5; carbide, 12385-15-8.

Supplementary Material Available: Listings of cation coordinates and thermal parameters for **1**–**3** (Tables SI, SIII, SV and SII, SIV, SVI) (13 pages); listings of observed and calculated structure factor amplitudes (78 pages). Ordering information is given on any current masthead page.